

JAERI - M
86-076

**STUDY OF THE SECOND HARMONIC ELECTRON
CYCLOTRON HEATING IN JFT-2M TOKAMAK**

(A REPORT PRESENTED AT JAPAN-US WORKSHOP ON
TRANSPORT PHENOMENA DURING RF HEATING AND
CURRENT DRIVE, KYOTO UNIV., 16-18 Dec. 1985)

May 1986

Katsumichi HOSHINO, Takumi YAMAMOTO, Hisato KAWASHIMA
Yoshihiko UESUGI, Satoshi KASAI, Tomohide KAWAKAMI
Tohru MATOBA, Toshiaki MATSUDA, Hiroshi MATSUMOTO
Yukitoshi MIURA, Masahiro MORI, Kazuo ODAJIMA
Hiroaki OGAWA, Toshihide OGAWA, Hideo OHTSUKA
Seio SENGOKU, Teruaki SHOJI, Norio SUZUKI, Hiroshi TAMAI
Toshihiko YAMAUCHI, Mitsuru HASEGAWA*, Susumu TAKADA**
and Akimasa FUNAHASHI

JAERI-M レポートは、日本原子力研究所が不定期に公刊している研究報告書です。

入手の問合わせは、日本原子力研究所技術情報部情報資料課（〒319-11 茨城県那珂郡東海村）あて、お申しこしてください。なお、このほかに財団法人原子力弘済会資料センター（〒319-11 茨城県那珂郡東海村日本原子力研究所内）で複写による実費頒布をおこなっております。

JAERI-M reports are issued irregularly.

Inquiries about availability of the reports should be addressed to Information Division, Department of Technical Information, Japan Atomic Energy Research Institute, Tokai-mura, Naka-gun, Ibaraki-ken 319-11, Japan.

© Japan Atomic Energy Research Institute, 1986

編集兼発行 日本原子力研究所
印刷 山田 軽印刷所

Study of the Second Harmonic Electron Cyclotron Heating
in JFT-2M Tokamak

Katsumichi HOSHINO, Takumi YAMAMOTO, Hisato KAWASHIMA
Yoshihiko UESUGI, Satoshi KASAI, Tomohide KAWAKAMI
Tohru MATOBA, Toshiaki MATSUDA, Hiroshi MATSUMOTO
Yukitoshi MIURA, Masahiro MORI, Kazuo ODAJIMA
Hiroaki OGAWA, Toshihide OGAWA, Hideo OHTSUKA
Seio SENGOKU, Teruaki SHOJI, Norio SUZUKI
Hiroshi TAMAI, Toshihiko YAMAUCHI, Mitsuru HASEGAWA*
Susumu TAKADA** and Akimasa FUNAHASHI

Department of Thermonuclear Fusion Research
Naka Fusion Research Establishment, JAERI
Japan Atomic Energy Research Institute
Tokai-mura, Naka-gun, Ibaraki-ken

(Received April 24, 1986)

Initial experimental results on the energy confinement time and phenomena related to the particle confinement during the 60 GHz second harmonic electron cyclotron heating (ECH) on JFT-2M tokamak are reported.

keywords : JFT-2M Tokamak, Electron Cyclotron Heating, Confinement Time, Particle Confinement

* On leave from Mitsubishi Electric Co.

** On leave from Mitsubishi Electric Computer Systems Tokyo Co.

A report presented at Japan-US Workshop on Transport Phenomena During RF Heating and Current Drive, Kyoto Univ., 16-18 Dec. 1985.

JFT-2Mトカマクの二倍高調波電子サイクロロン加熱の研究

日本原子力研究所那珂研究所核融合研究部プラズマ実験研究室

星野 克道・山本 巧・川島 寿人・上杉 喜彦
河西 敏・河上 知秀・的場 徹・松田 俊明
松本 宏・三浦 幸俊・森 雅博・小田島和男
小川 宏明・小川 俊英・大塚 英男・仙石 盛夫
荘司 昭朗・鈴木 紀男・玉井 広史・山内 俊彦
長谷川 満*・高田 晋**・船橋 昭昌

(1986年4月24日受理)

JFT-2Mトカマクの60 GHz_z二倍高調波電子サイクロロン加熱(ECH)の初期実験時のエネルギー閉じ込め時間の評価および粒子閉じ込めに関連する現象について報告を行なう。(これは、「高周波加熱と電流駆動中の輸送現象に関する日米ワークショップ」京都大学, 1985年12月16日~18日に於ける報告内容である。)

那珂研究所：茨城県那珂郡那珂町大字向山

* 三菱電機㈱

** 三菱電機東部コンピュータシステム㈱

「高周波加熱と電流駆動中の輸送現象に関する日米ワークショップ」京都大学, 1985年12月16日~18日に於ける報告である。

Contents

1. ECH Experiment at JAERI	1
2. 60 GHz RF Transmission System	1
3. Experimental Results and Discussions	2
3.1 Density Dependence of Electron Heating	2
3.2 Power Dependence of Electron Heating	3
3.3 Dependence on the Position of the Second Harmonic ECR Layer	3
3.4 Profiles $T_e(r)$, $n_e(r)$ During ECH	3
3.5 Estimation of Stored Energy and Energy Confinement Time	3
3.6 Change of the Current Profile by ECH (Estimation of l_i)	6
3.7 Density Drop Associated with ECH	6
4. Summary	7
Acknowledgement	7
References	8

目 次

1. 日本原子力研究所に於けるECH実験の経緯	1
2. 60GHz高周波伝送系	1
3. 実験結果と議論	2
3.1 電子加熱の密度依存性	2
3.2 電子加熱の高周波パワー依存性	3
3.3 二倍高周波電子サイクロトロン共鳴層の位置に対する依存性	3
3.4 電子サイクロトロン共鳴加熱中の分布 $T_e(r)$, $N_e(r)$	3
3.5 蓄積エネルギーとエネルギー閉じ込め時間の評価	3
3.6 電子サイクロトロン共鳴加熱による電流分布の変化 (I_i の評価)	6
3.7 電子サイクロトロン共鳴加熱に伴う密度減少	6
4. ま と め	7
謝 辞	7
参考文献	8

1. ECH Experiment at JAERI

Study of the electron cyclotron heating (ECH) started on JFT-2 tokamak in 1980-81 at JAERI (Table 1). JFT-2 tokamak had major radius $R = 0.90$ m and minor radius $a = 0.25$ m. We studied 28 GHz fundamental ($\omega = \Omega_{ce}$) ECH by launching three kinds of modes from different antennas. The experiment was carried out in a collaboration with GA Technologies Inc. in USA. The extraordinary mode (X-mode) was launched from the high field side of the torus (inside launch), and the ordinary mode (O-mode) was launched from outside and TE_{02} mode was launched from the top of the torus. The plasma heating by these modes was studied¹⁾⁻⁴⁾.

We made a design study of a new 60 GHz ECH system in 1982-83⁵⁾, and the system with one gyrotron (Varian VGE-8060) was completed in 1984⁶⁾. The second harmonic wave was first launched into JFT-2M tokamak in Nov.-Dec. 1984. JFT-2M tokamak is a non-circular tokamak of $R = 1.31$ m and $a \times b = 0.35$ m \times 0.55 m. X-mode with parallel refractive index $n_{\parallel} = 0.17$ (the angle between the wave vector and magnetic field vector is 80°) was launched from outside, and ECH of rf sustained tokamak plasma by the lower hybrid wave was studied⁶⁾⁻⁸⁾.

In this September, we made a measurement of electron temperature profile and density profile.

We are going to report about the experimental results concerning to the transport phenomena during the second harmonic ECH of JFT-2M tokamak.

In the end of this December, a power up of the ECH system to 400 kW will be completed by adding one more gyrotron to the system. And we are going to study fast wave current drive with a high temperature plasma obtained by ECH in the next year (1986).

2. 60 GHz RF Transmission System

A schematic diagram⁶⁾ of the 60 GHz ECH system is given in Fig. 1. The circular TE_{02} mode generated by the gyrotron is mode-converted to circular TE_{01} mode which has a low transmission loss in a circular waveguide. Finally, the TE_{01} mode is mode-converted to quasi-linearly polarized TE_{11} mode by a mode converter in the tokamak vacuum chamber. The TE_{11} mode is launched from a conical horn antenna which has 50 mm

1. ECH Experiment at JAERI

Study of the electron cyclotron heating (ECH) started on JFT-2 tokamak in 1980-81 at JAERI (Table 1). JFT-2 tokamak had major radius $R = 0.90$ m and minor radius $a = 0.25$ m. We studied 28 GHz fundamental ($\omega = \Omega_{ce}$) ECH by launching three kinds of modes from different antennas. The experiment was carried out in a collaboration with GA Technologies Inc. in USA. The extraordinary mode (X-mode) was launched from the high field side of the torus (inside launch), and the ordinary mode (O-mode) was launched from outside and TE_{02} mode was launched from the top of the torus. The plasma heating by these modes was studied¹⁾⁻⁴⁾.

We made a design study of a new 60 GHz ECH system in 1982-83⁵⁾, and the system with one gyrotron (Varian VGE-8060) was completed in 1984⁶⁾. The second harmonic wave was first launched into JFT-2M tokamak in Nov.-Dec. 1984. JFT-2M tokamak is a non-circular tokamak of $R = 1.31$ m and $a \times b = 0.35$ m \times 0.55 m. X-mode with parallel refractive index $n_{\parallel} = 0.17$ (the angle between the wave vector and magnetic field vector is 80°) was launched from outside, and ECH of rf sustained tokamak plasma by the lower hybrid wave was studied⁶⁾⁻⁸⁾.

In this September, we made a measurement of electron temperature profile and density profile.

We are going to report about the experimental results concerning to the transport phenomena during the second harmonic ECH of JFT-2M tokamak.

In the end of this December, a power up of the ECH system to 400 kW will be completed by adding one more gyrotron to the system. And we are going to study fast wave current drive with a high temperature plasma obtained by ECH in the next year (1986).

2. 60 GHz RF Transmission System

A schematic diagram⁶⁾ of the 60 GHz ECH system is given in Fig. 1. The circular TE_{02} mode generated by the gyrotron is mode-converted to circular TE_{01} mode which has a low transmission loss in a circular waveguide. Finally, the TE_{01} mode is mode-converted to quasi-linearly polarized TE_{11} mode by a mode converter in the tokamak vacuum chamber. The TE_{11} mode is launched from a conical horn antenna which has 50 mm

in diameter. The radiated microwave beam has a small beam divergence. The full beam width (full half width at -3 dB point) at the center of the vacuum chamber is 7 cm. The total length of the rf transmission system is 32.9 m. One can launch either X-mode ($\vec{E} \perp \vec{B}$) or O-mode ($\vec{E} // \vec{B}$) by rotating the TE₀₁-TE₁₁ mode converter. The efficiency of the transfer of the microwave from TE₀₂ mode directional coupler to the final conical horn antenna is 50 %. The loss in the three corrugated bends was unexpectedly large. Therefore we are going to make an improvement of the bends.

3. Experimental Results and Discussions

3.1 Density Dependence of the Electron Heating

Density dependence of the measured increase in the center electron temperature $\Delta T_e(0)$ measured by the soft X-ray energy analysis, and density dependence of the increase in $\Lambda + \frac{1}{2} \equiv \beta_p + \frac{l_i}{2} - \frac{1}{2}$ (β_p : poloidal beta value, and $l_i = \frac{4\pi}{\mu_0} \times$ [internal self inductance per unit length of plasma]) which was measured from the equilibrium poloidal field, are shown in Fig. 2. This is a case that the electron cyclotron resonance (ECR) layer locates at the plasma center (center resonance case). As seen in the figure, at $\bar{n}_e = 1.80 \times 10^{19} \text{ m}^{-3}$ (line average density measured by microwave interferometer), the increase of the center electron temperature $\Delta T_e(0)$ is negligible, and $\Lambda + \frac{1}{2}$ decreases by the ECH pulse. These phenomena are explained by the appearance of the cutoff region in the core of the plasma. The typical density profile of the JFT-2M tokamak is expressed by $n_e(r) = n_e(0) (1 - r^2/a^2)^{\alpha_n}$ with $\alpha_n = 1-2$. Then the relation between the local density $n_e(0)$ and line average density \bar{n}_e is written as $n_e(0) = (1.5 \sim 1.8)\bar{n}_e$. The calculated local cutoff density of the right hand wave (f_R cutoff) is $n_{C,R} = 2.23 \times 10^{19} \text{ m}^{-3}$. By equating $n_e(0) = n_{C,R}$, one obtains the cutoff density of $\bar{n}_e = (1.24 - 1.49) \times 10^{19} \text{ m}^{-3}$ in the case of $\alpha_n = 1-2$ for the X-mode. Similarly, the cutoff density of the O-mode which is provided by the plasma cutoff (f_p) is $\bar{n}_e = (2.48 - 2.97) \times 10^{19} \text{ m}^{-3}$. The cutoff density thus obtained is indicated by arrows in the abscissa of Fig. 2. The experimental data show that core heating is negligible above the core cutoff density of the X-mode. Thus the wave cutoff occurs at the right hand wave cutoff in consistent with the cold plasma theory. We do not observe

in diameter. The radiated microwave beam has a small beam divergence. The full beam width (full half width at -3 dB point) at the center of the vacuum chamber is 7 cm. The total length of the rf transmission system is 32.9 m. One can launch either X-mode ($\vec{E} \perp \vec{B}$) or O-mode ($\vec{E} // \vec{B}$) by rotating the TE₀₁-TE₁₁ mode converter. The efficiency of the transfer of the microwave from TE₀₂ mode directional coupler to the final conical horn antenna is 50 %. The loss in the three corrugated bends was unexpectedly large. Therefore we are going to make an improvement of the bends.

3. Experimental Results and Discussions

3.1 Density Dependence of the Electron Heating

Density dependence of the measured increase in the center electron temperature $\Delta T_e(0)$ measured by the soft X-ray energy analysis, and density dependence of the increase in $\Lambda + \frac{1}{2} \equiv \beta_p + \frac{1}{2} - \frac{1}{2}$ (β_p : poloidal beta value, and $l_i = \frac{4\pi}{\mu_0} \times$ [internal self inductance per unit length of plasma]) which was measured from the equilibrium poloidal field, are shown in Fig. 2. This is a case that the electron cyclotron resonance (ECR) layer locates at the plasma center (center resonance case). As seen in the figure, at $\bar{n}_e = 1.80 \times 10^{19} \text{ m}^{-3}$ (line average density measured by microwave interferometer), the increase of the center electron temperature $\Delta T_e(0)$ is negligible, and $\Lambda + \frac{1}{2}$ decreases by the ECH pulse. These phenomena are explained by the appearance of the cutoff region in the core of the plasma. The typical density profile of the JFT-2M tokamak is expressed by $n_e(r) = n_e(0) (1 - r^2/a^2)^{\alpha_n}$ with $\alpha_n = 1-2$. Then the relation between the local density $n_e(0)$ and line average density \bar{n}_e is written as $n_e(0) = (1.5 \sim 1.8)\bar{n}_e$. The calculated local cutoff density of the right hand wave (f_R cutoff) is $n_{C,R} = 2.23 \times 10^{19} \text{ m}^{-3}$. By equating $n_e(0) = n_{C,R}$, one obtains the cutoff density of $\bar{n}_e = (1.24 - 1.49) \times 10^{19} \text{ m}^{-3}$ in the case of $\alpha_n = 1-2$ for the X-mode. Similarly, the cutoff density of the O-mode which is provided by the plasma cutoff (fp) is $\bar{n}_e = (2.48 - 2.97) \times 10^{19} \text{ m}^{-3}$. The cutoff density thus obtained is indicated by arrows in the abscissa of Fig. 2. The experimental data show that core heating is negligible above the core cutoff density of the X-mode. Thus the wave cutoff occurs at the right hand wave cutoff in consistent with the cold plasma theory. We do not observe

any core plasma heating above the cutoff density by launching the second harmonic X-mode from the low field side of the torus.

3.2 Power Dependence of Electron Heating

Power dependence of $\Delta T_e(0)$ and $\Delta(\beta_p + 1/2)$ is shown in Fig. 3. It is the center resonance case. As shown, $\Delta T_e(0)$ is linear in the ECH power up to $P_{ECH} = 80$ kW.

3.3 Dependence on the Position of the Second Harmonic ECR Layer

A drastic change in $\Delta(\Lambda + 1/2)$ is observed when the position of the second harmonic ECR layer is varied (Fig. 4). In the center resonance case ($r_{res} = 0$ cm), $\Delta(\Lambda + 1/2) > 0$. But in the off-center resonance case ($r_{res} = 15$ cm, -18 cm), $\Delta(\Lambda + 1/2) < 0$. Thus $\Lambda + 1/2 \equiv \beta_p + \frac{1}{2} - \frac{1}{2}$ decreases by the off-center heating. Then a question arises whether β_p (or stored energy W) decreases by the off-center heating or not. As we do not have the diamagnetic measurement*, we made a measurement of the profiles $T_e(r)$, $n_e(r)$ by a Thomson scattering system, ECE system and soft X-ray system.

3.4 Profiles $T_e(r)$, $n_e(r)$ During ECH

Measured profiles of electron temperature $T_e(r)$ and density $n_e(r)$ are given in Figs. 5(a) and (b). The position of the ECR layer is shown by an arrow. In the center resonance case (Fig. 5(a)), electron temperature profile exhibits peaking in the core region. whereas, in the off-center resonance case (Fig. 5(b)), the profile becomes broad. The laser profile is obtained by accumulating 10 shots to decrease the statistical error because of the weakness of the scattered laser light. The measured density points have a considerable scatterings in spite of the accumulation of 10 shots.

3.5 Estimation of the Stored Energy and Energy Confinement Time

In this section, stored energy W (kJ) and energy confinement time

* Diamagnetic measurement was not available last year (1985). But a diamagnetic measurement has come into operation since the beginning of this year (1986). And it was found that the conclusion stated below is correct.

τ_E (ms) are estimated using the measured profiles of the previous section (Fig. 5).

Those profiles are fitted well by the following function of the form $f(r) = f(0)(1-r^2/a^2)^\alpha$, where r is the minor radial coordinate, a is the minor radius ($a = 33$ cm) and α is the power index of the profile function. Though there is no measured profile in the region 22.5 cm $< r \leq 33$ cm, we make an assumption that the profiles are expressed by the former function.

The following functions are taken for the estimation.

(1) joule plasma

$$T_e(r) = T_e(0)_j (1-r^2/a^2)^{\alpha_{T,j}}$$

$$n_e(r) = n_e(0)_j (1-r^2/a^2)^{\alpha_{n,j}}$$

where $T_e(0)_j = 550 \pm 50$ eV, $n_e(0)_j = 1.50 \times 10^{19} \text{ m}^{-3}$, $a = 0.33$ m,

$$\alpha_{T,j} = 2.5, \alpha_{n,j} = 1.2.$$

(2) with ECH

(2-1) center resonance case ($B_{t0} = 1.07$ T, $r_{\text{res}} = 0$ cm)

$$T_e(r) = T_e(0)_{\text{rf}} (1-r^2/a^2)^{\alpha_{T,\text{rf1}}} \quad (0 \leq r \leq 11)$$

$$T_e(0)_j (1-r^2/a^2)^{\alpha_{T,\text{rf2}}} \quad (11 < r \leq 33)$$

$$n_e(r) = n_e(0)_{\text{rf}} (1-r^2/a^2)^{\alpha_{n,\text{rf}}}$$

where $T_e(0)_{\text{rf}} = 950$ eV, $T_e(0)_j = 550$ eV, $n_e(0)_{\text{rf}} = 1.44 \times 10^{19} \text{ m}^{-3}$,

$$\alpha_{T,\text{rf1}} = 7.0, \alpha_{T,\text{rf2}} = 2.3, \alpha_{n,\text{rf}} = 1.2.$$

(2-2) off-center resonance case ($B_{t0} = 1.19$ T, $r_{\text{res}} = 15$ cm)

$$T_e(r) = T_e(0)_{\text{rf1}} (1-r^2/a^2)^{\alpha_{T,\text{rf1}}} \quad (0 \leq r \leq 11)$$

$$T_e(0)_{\text{rf2}} (1-r^2/a^2)^{\alpha_{T,\text{rf2}}} \quad (11 < r \leq 33)$$

$$n_e(r) = n_e(0)_{\text{rf}} (1-r^2/a^2)^{\alpha_{n,\text{rf}}}$$

where $T_e(0)_{\text{rf1}} = 550$ eV, $T_e(0)_{\text{rf2}} = 700$ eV, $n_e(0) = 1.41 \times 10^{19} \text{ m}^{-3}$,

$$\alpha_{T,\text{rf1}} = 1.0, \alpha_{T,\text{rf2}} = 2.8, \alpha_{n,\text{rf}} = 1.2.$$

From these profiles, one can calculate the stored energy in the electron species as,

$$W_{e,j} = 6 \pi^2 R \int_0^a n_e(r) T_e(r) r dr$$

$$= 3 \pi^2 R a^2 \frac{n_e(0)_j T_e(0)_j}{\alpha_{n,j} + \alpha_{T,j} + 1} \quad (\text{for joule plasma})$$

$$W_{e,rf} = 6 \pi^2 R \left[T_e(0)_{rf1} n_e(0)_{rf1} \int_0^{r_1} (1-r^2/a^2)^{\alpha_{t,rf1} + \alpha_{n,rf}} r dr \right. \\ \left. + T_e(0)_{rf2} n_e(0)_{rf2} \int_{r_1}^a (1-r^2/a^2)^{\alpha_{T,rf2} + \alpha_{n,rf}} r dr \right]$$

$$\text{with } \int_{r_1}^{r_2} (1-r^2/a^2)^\alpha r dr = -\frac{a^2}{2} \frac{1}{\alpha+1} \left\{ \left(1 - \frac{r_2^2}{a^2}\right)^{\alpha+1} - \left(1 - \frac{r_1^2}{a^2}\right)^{\alpha+1} \right\}$$

(during ECH).

The calculated stored energy in the electron species W_e is given in Table 2. As shown, the stored energy W_e increases even in the off-center resonance case*. The central ion temperature $T_i(0)$ stays constant at $T_i(0) = 300 \pm 20$ eV by a charge exchange measurement. Therefore, we set the stored energy in the ion species as almost constant by ECH except a slight decrease due to the decrease in plasma density \bar{n}_e . The joule input power decreases during rf, because loop voltage drops by the increase in the electron temperature. The energy confinement time thus obtained $\tau_{E,nT}$ is given in Table 2. On the other hand, one can estimate the joule stored energy and hence the joule confinement time $\tau_{E,\Lambda}$ from $\Lambda+1/2$ by changing the plasma density and taking the gradient of $\Lambda+1/2$ with respect to the density. $\frac{\partial \Lambda}{\partial n_e} \cong \frac{\partial \beta_p}{\partial n_e}$. Here we assume that $l_i = \text{const}$ against a small change in density. By integrating $\frac{\partial \beta_p}{\partial n_e}$ over density, one can obtain W . The energy confinement time of the joule plasma thus obtained $\tau_{E,\Lambda}$ is also given in Table 2. The energy confinement time of the joule plasma by these two methods almost agrees, $\tau_{E,nT} \cong \tau_{E,\Lambda}$. We notice that the energy confinement time is almost the same between the center resonance case and off-center resonance case ($r_{\text{res}}/a = 0.46$, safety factor $q_a = 5$). Here we assumed that all of the launched ECH power is absorbed completely by the plasma in the calculation of the energy confinement time.

* This result was confirmed by the recent measurement of diamagnetism. The stored energy increases in spite of the decrease in $\Lambda+1/2$ in the off-center resonance heating.

The calculated single path absorption rate at the second harmonic ECR layer⁶⁾ is shown in Fig. 6. In the center resonance case $P_{ab}/P \cong 0.92$ and in the off-center resonance case $P_{ab}/P \cong 0.75$. If the absorption occurs only in single path across the ECR layer, difference in the energy confinement time in these two cases vanishes as shown in Table 2 ($\tau_{E,nT}$ enclosed by brackets).

3.6 Change of the Current Profile by ECH (Estimation of l_i)

As described in the previous section, the plasma stored energy W increases both for the center resonance case and off-center resonance case. This fact means that β_p of both cases increases by ECH. Whereas $\Lambda + 1/2$ ($\equiv \beta_p + \frac{l_i}{2} - \frac{1}{2}$) decreases in the off-center resonance case. This means that l_i decreases in the off-center resonance case. The effect of the horizontal displacement to the l_i is negligible because the plasma position is controlled by a feed back circuit. Then the decrease in l_i is the result of the broadening of the current profile. Therefore a broadening of the current profile occurs by the off-center ECH.

The result of the estimation of l_i in the off-center resonance case is given in Table 3. The rate of decrease in l_i is $\Delta l_i = -0.22/60$ ms.

The decrement in $\Lambda + 1/2$ does not saturate in the ECH pulse length of 100 ms.

3.7 Density Drop Associated with ECH

Density drop which was observed in 28 GHz fundamental ECH is also observed in the second harmonic ECH of JFT-2M tokamak. Parameter dependence of the density drop $-\Delta \bar{n}_e$ is shown in Fig. 7. The drop $-\Delta \bar{n}_e$ increases with the ECH power (Fig. 7(a)), plasma density (Fig. 7(b)) and almost independent of the plasma current (Fig. 7(c)). The time behaviour of the line average density is shown in Fig. 8. Density drop is small in the center resonance case (Fig. 8(a)) and saturates quickly. In the off-center resonance case (Fig. 8(b)), the density drop is large and does not saturate in 100 ms.

Thus, in the limiter discharge, the density drop occurs by the application of ECH in the JFT-2M tokamak. On the other hand, in ECH of the Doublet III tokamak (expanded boundary, 60 GHz, $\omega = \Omega_{ce}$, X-mode),

density drop is not so large. These facts show that the density drop is largely related to the plasma edge condition. Therefore it seems that the direct outward diffusion due to the rf wave does not take a main role in the density drop phenomena by ECH.

The time scale of the phenomena is more than 100 ms. The time scale is the order of the diffusion time of the magnetic field diffusion. Therefore it suggests that particle confinement and temperature/current profile which are changing as described above, have some close relations.

4. Summary

- (1) The electron-temperature/current profile changes with the position of the ECR layer.
- (2) The energy confinement time does not differ much between the center resonance case and off-center resonance case. This result is similar to those of the other machines such T-10 or Doublet III.
- (3) Density drop seems to be related largely to the plasma profile or periphery condition, and not to the direct outward diffusion by the rf wave.
- (4) In the ECH experiment, the stored energy can not be obtained from the equilibrium poloidal magnetic field $\Lambda + 1/2$, because profile or l_1 changes by ECH. Diamagnetic measurement is essential for the estimation of the stored energy. (Diamagnetic measurement has already come into operation in JFT-2M tokamak. And it is found that these result stated above is consistent with the diamagnetic measurement, the result of which will be reported elsewhere.)

Acknowledgement

The authors are grateful to the operation groups of JFT-2M tokamak. They wish to acknowledge Drs. Y. Tanaka, M. Tanaka, M. Yoshikawa, K. Tomabechi, Y. Iso and S. Mori for their continuous encouragements.

density drop is not so large. These facts show that the density drop is largely related to the plasma edge condition. Therefore it seems that the direct outward diffusion due to the rf wave does not take a main role in the density drop phenomena by ECH.

The time scale of the phenomena is more than 100 ms. The time scale is the order of the diffusion time of the magnetic field diffusion. Therefore it suggests that particle confinement and temperature/current profile which are changing as described above, have some close relations.

4. Summary

- (1) The electron-temperature/current profile changes with the position of the ECR layer.
- (2) The energy confinement time does not differ much between the center resonance case and off-center resonance case. This result is similar to those of the other machines such T-10 or Doublet III.
- (3) Density drop seems to be related largely to the plasma profile or periphery condition, and not to the direct outward diffusion by the rf wave.
- (4) In the ECH experiment, the stored energy can not be obtained from the equilibrium poloidal magnetic field $\Lambda + 1/2$, because profile or I_i changes by ECH. Diamagnetic measurement is essential for the estimation of the stored energy. (Diamagnetic measurement has already come into operation in JFT-2M tokamak. And it is found that these result stated above is consistent with the diamagnetic measurement, the result of which will be reported elsewhere.)

Acknowledgement

The authors are grateful to the operation groups of JFT-2M tokamak. They wish to acknowledge Drs. Y. Tanaka, M. Tanaka, M. Yoshikawa, K. Tomabechi, Y. Iso and S. Mori for their continuous encouragements.

density drop is not so large. These facts show that the density drop is largely related to the plasma edge condition. Therefore it seems that the direct outward diffusion due to the rf wave does not take a main role in the density drop phenomena by ECH.

The time scale of the phenomena is more than 100 ms. The time scale is the order of the diffusion time of the magnetic field diffusion. Therefore it suggests that particle confinement and temperature/current profile which are changing as described above, have some close relations.

4. Summary

- (1) The electron-temperature/current profile changes with the position of the ECR layer.
- (2) The energy confinement time does not differ much between the center resonance case and off-center resonance case. This result is similar to those of the other machines such T-10 or Doublet III.
- (3) Density drop seems to be related largely to the plasma profile or periphery condition, and not to the direct outward diffusion by the rf wave.
- (4) In the ECH experiment, the stored energy can not be obtained from the equilibrium poloidal magnetic field $\Lambda + 1/2$, because profile or l_1 changes by ECH. Diamagnetic measurement is essential for the estimation of the stored energy. (Diamagnetic measurement has already come into operation in JFT-2M tokamak. And it is found that these result stated above is consistent with the diamagnetic measurement, the result of which will be reported elsewhere.)

Acknowledgement

The authors are grateful to the operation groups of JFT-2M tokamak. They wish to acknowledge Drs. Y. Tanaka, M. Tanaka, M. Yoshikawa, K. Tomabechi, Y. Iso and S. Mori for their continuous encouragements.

References

- 1) LaHaye R.J., Moeller C.P., Funahashi A., Yamamoto T., Hoshino K., Suzuki N., Wolfe S.M., Efthimion P.C., Toyama H. and Roh T: Nucl. Fusion 21, 1425 (1981).
- 2) Moeller C.P., Chan V.S., LaHaye R.J., Prater R., Yamamoto T., Funahashi A., Hoshino K. and Yamauchi T.: Phys. Fluids 25, 1211 (1982).
- 3) Prater R. and Moeller C.P.: Proc. of Third Joint Varenna-Grenoble Int. Symp. on Heating Toroidal Plasmas, 635 (1982).
- 4) Hoshino K., Yamamoto T., Funahashi A., Suzuki N., Matoba T., Yamauchi T., Matsumoto H., Kawakami T., Kimura H., Konoshima S., Maeno M. et al.: J. Phys. Soc. Jpn. 54, 2503 (1985).
- 5) Hoshino K., Kawashima H., Hata K. and Yamamoto T.: JAERI-M Report 83-148 Sept. (1983).
- 6) Hoshino K., Yamamoto T., Kawashima H., Shibata T. and Shibuya T.: JAERI-M Report 85-169 (1985).
- 7) Hoshino K., Yamamoto T., Suzuki N., Uesugi Y., Kawashima H., Matoba T., Kasai S., Kawakami T., Maeno M., Matsuda T., Matsumoto H., Miura Y., et al.: in Proc. of the 12th European Conf. on Controlled Fusion and Plasma Physics, Budapest, Hungary, vol. 9F part 2 p.184 (1985).
- 8) Yamamoto T., Hoshino K., Uesugi Y., Kawashima H., et al.: submitted to Phys. Rev. Lett..

Table 1 ECH Experiment at JAERI.

ECH Experiment at JAERI

1980-1981 JFT-2 Tokamak (R=0.9m, a=0.25m)
 f=28GHz, 200kW
 $\omega = \omega_{ce}$
 { X-mode (inside launch)
 O-mode (outside launch)
 TE₀₂ mode (top launch)

1984 Nov.-Dec. JFT-2M Tokamak (R=1.31m, a=0.35m)
 f=60GHz, 200kW
 $\omega = 2\omega_{ce}$
 X-mode (outside launch)
 $n_{//} = 0.17$ ($\theta = 80^\circ$)
 @ ECH of LHW sustained tokamak plasma

1985 Sept. Profile Measurement $\Gamma_e(r), n_e(r)$

 Dec. Power up to 400kW
 1986- @Fast wave current drive + ECH

Table 2 Estimation of the stored energy W and energy confinement time during ECH.

	$T_e(0)$ (eV)	$n_e(0)$ ($10^{19} m^{-3}$)	α_T #	α_n	W_e (kJ)	W_i (kJ)	P_j (kW)	$\tau_{E,nT}$	$\tau_{E,\Lambda}^*$
joule plasma	550 ₋₅₀ ⁺⁵⁰	1.50 _{-0.1} ^{+0.1}	2.5 _{-0.1} ^{+0.1}	1.2 _{-0.1} ^{+0.1}	1.33 _{-0.1} ^{+0.1}	0.73 _{-0.1} ^{+0.1}	150 ₋₅ ⁺⁵	14 ₋₁ ⁺¹	12 ₋₁ ⁺¹
with ECH	950		7.0(r<.11)	1.2					
cent. res. (P _{ab} /P=.92)	550	1.44	2.3(r>.11)		1.54	0.70	110 ₋₅ ⁺⁵	12	(12)
off-cent. resonance	550		1.0(r<.11)	1.2					
(P _{ab} /P=.75)	700	1.41	2.8(r>.11)		1.40	0.70	120 ₋₅ ⁺⁵	11	(12)

* use β_p obtained from the slope of Λ with respect to density assuming that l_i is constant against the small change of density.

** $P_{ECH} = 80kW, I_p = 100kA \rightarrow P_{ECH}/P_j = .7$

*** $T_i(0) = 300 \pm 20eV$ by CX measurement. no increase by ECH.

@ Energy confinement times of joule plasma by the two methods almost agrees; $\tau_{E,nT} \approx \tau_{E,\Lambda}$

@ With the correction of the single path absorption rate, the energy confinement time is almost the same for center resonance case and off-center resonance case.

α is the index of the fitting function of the profiles;
 $f(r) = f(0) (1 - r^2/a^2)^\alpha$

Table 3 Estimation of l_i . Suffix j indicates the value for the joule plasma and rf for during ECH.

Change of the current profile
by ECH (change in l_i)

- * stored energy W_e increases both for the
 - { center resonance case
 - and
 - { off-center resonance case

+ β_p increases by ECH

- * But $\Lambda \approx \beta + l_i/2 - 1$ decreases in the
off-center l_i resonance case

+ l_i decreases by ECH

broadening in current profile $j(r)$ by
ECH

Λ_j	$\beta_{p,j}$	$l_{i,j}$	Λ_{rf}	$\beta_{p,rf}$	$l_{i,rf}$	<u>Δl_i</u>
.50	.30	1.40	.40	.31	1.18	<u>-.22</u>

60 GHz Transmission System for the JFT-2M Tokamak (Side view)

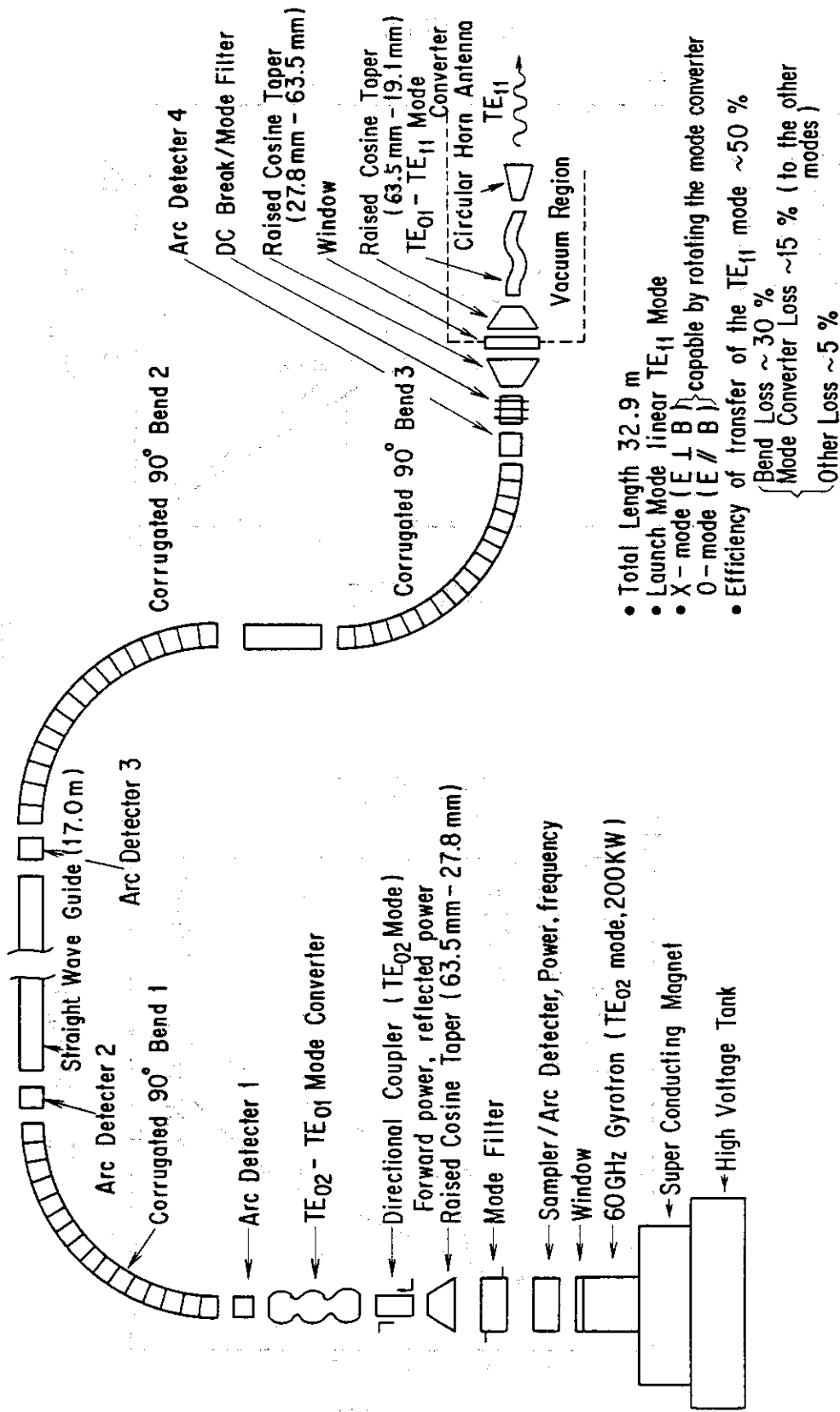


Fig. 1 60 GHz RF Transmission System for the JFT-2M Tokamak

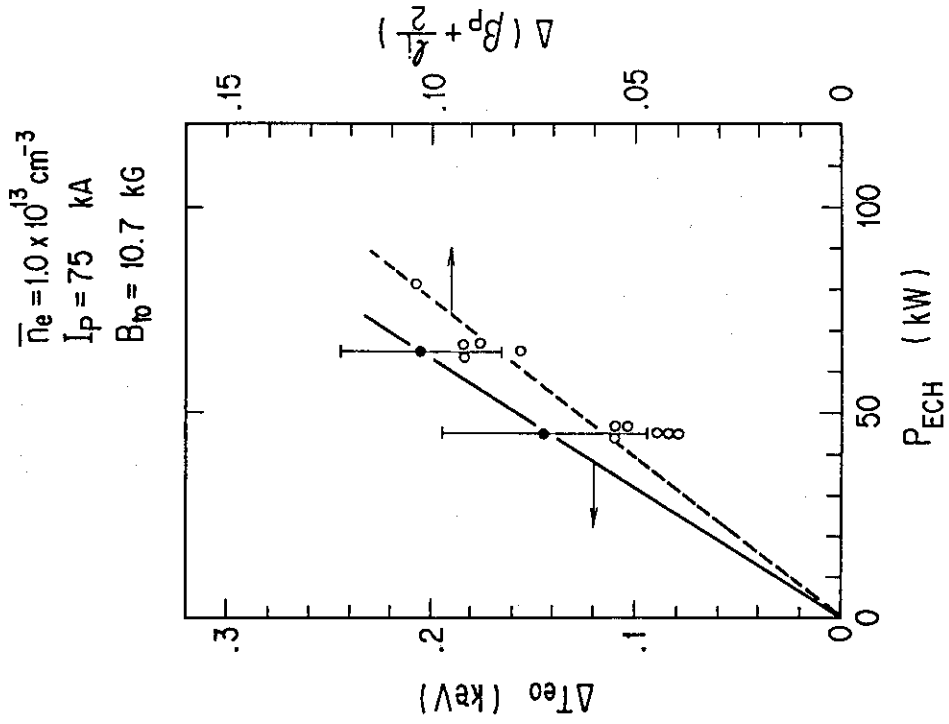


Fig. 3

Power dependence of $\Delta T_e(0)$ and $\Delta(\beta_p + 1/2)$ in the center resonance case.

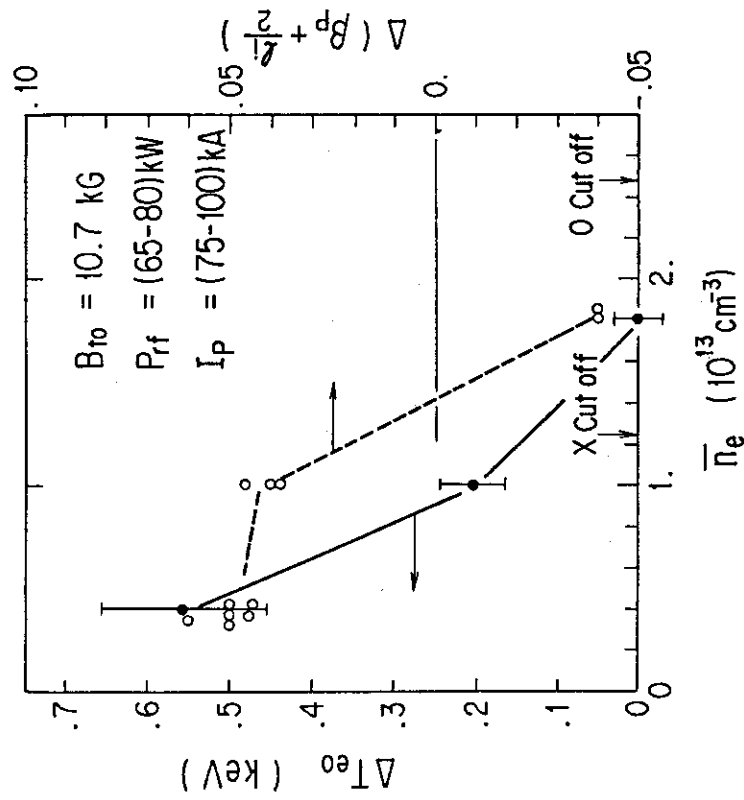


Fig. 2

Density dependence of increase in the center electron temperature $\Delta T_e(0)$ and increase in $\Delta + 1/2$, $\Delta(\beta_p + 1/2)$.

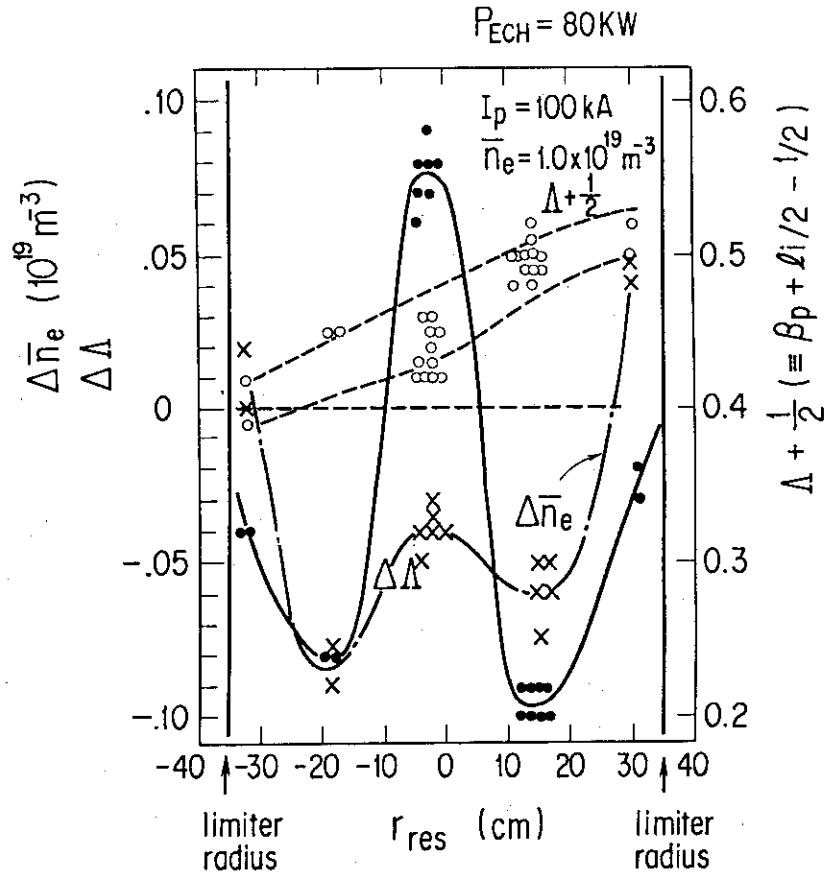


Fig. 4 Dependence of $\Delta\Lambda$, Λ and $-\Delta\bar{n}_e$ on the position of the second harmonic ECR layer.

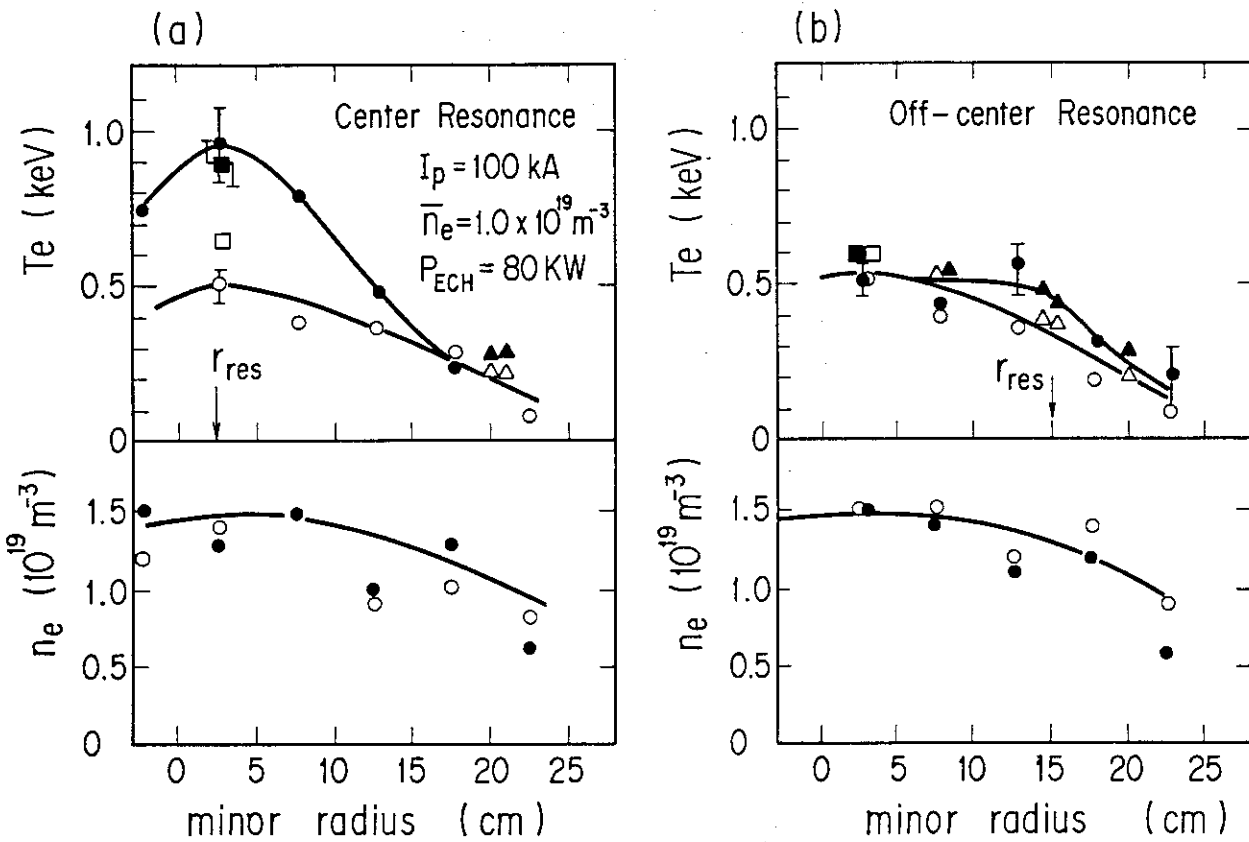


Fig. 5 Profiles of electron temperature and density for (a) center resonance case, and (b) off-center resonance case.

● --- Laser, ▲ --- ECE, ■ --- Soft X-ray.

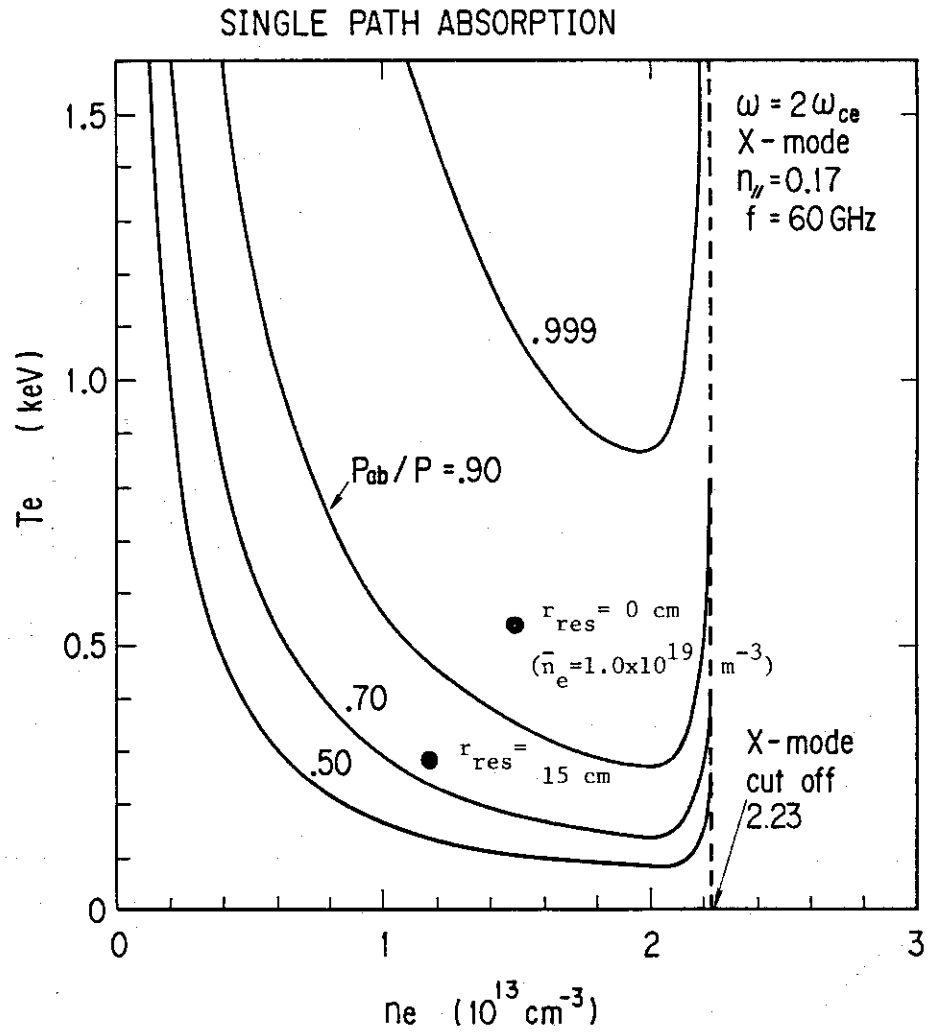


Fig. 6 Calculated single path absorption rate at the second harmonic ECR layer for the X-mode. frequency $f = 60 \text{ GHz}$, $n_{\parallel} = 0.17$.

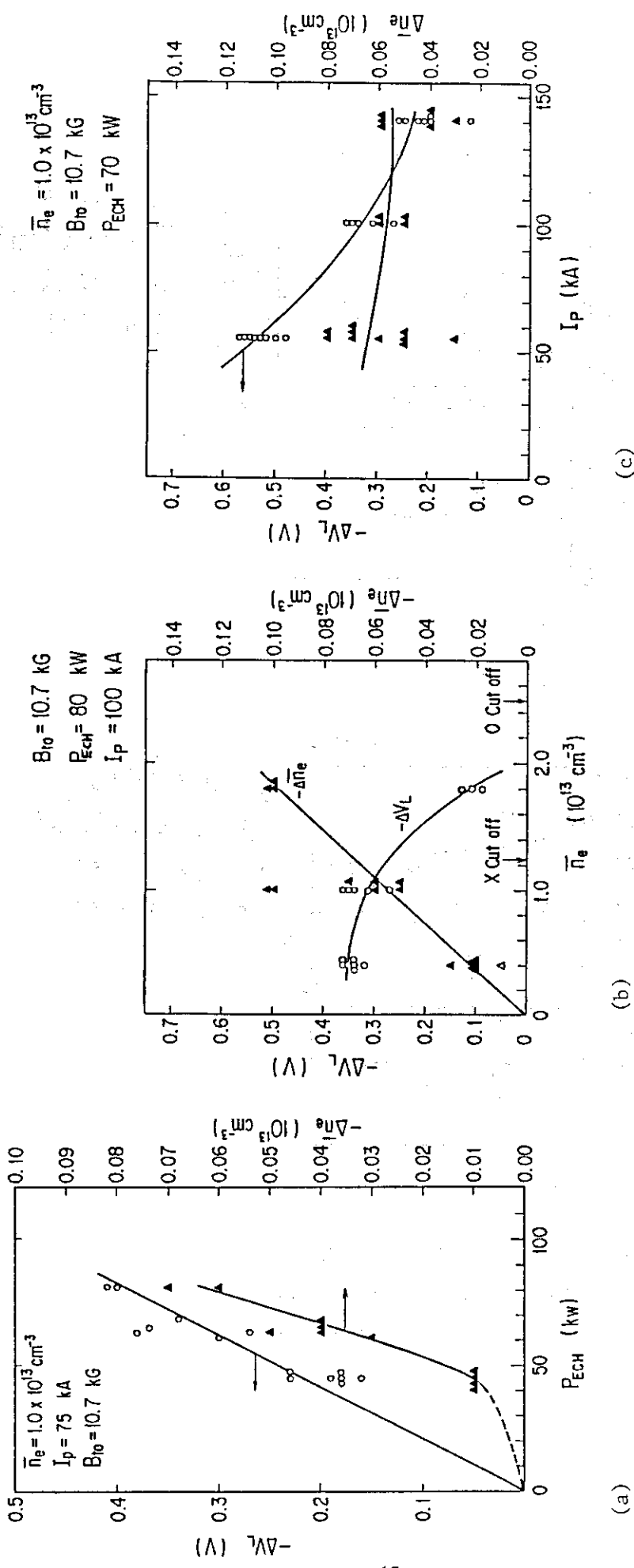


Fig. 7 Density drop associated with ECH of JFT-2M tokamak. (a) power dependence (b) density dependence (c) dependence on plasma current. center resonance case. Dependence on the position of the ECR layer is shown in Fig. 4.

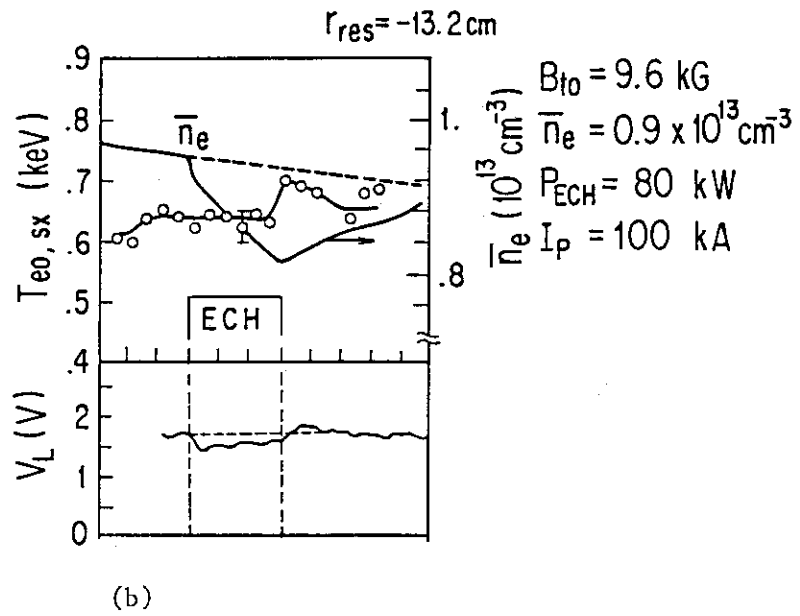
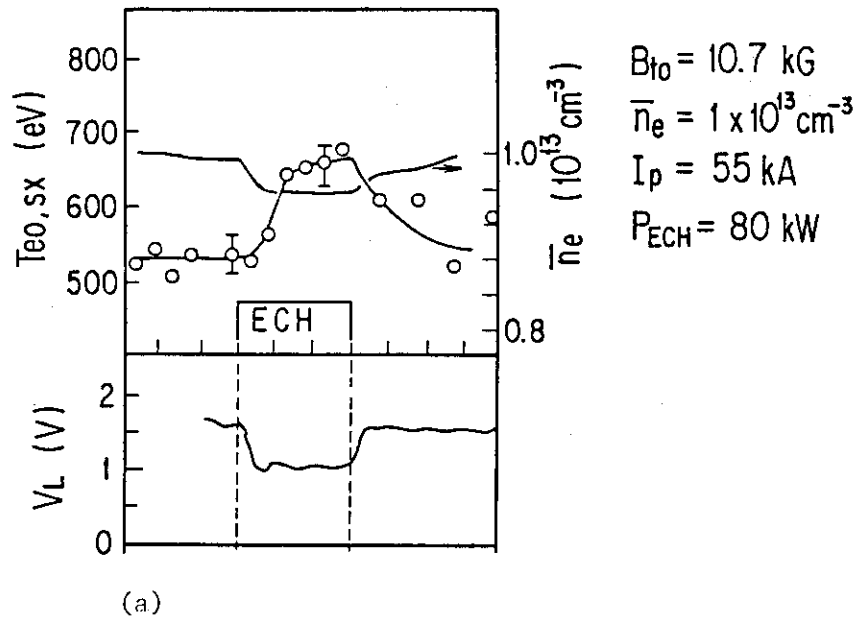


Fig. 8 Time behaviour of the density drop.
 (a) center resonance case,
 (b) off-center resonance case.